Fatigue Limit Evaluation of Various Martensitic Stainless Steels with New Robust Thermographic Data Analysis

(DOI): http://dx.doi.org/10.1016/j.ijfatigue.2014.12.010
Accepted Version- International Journal of Fatigue

FATIGUE LIMIT EVALUATION OF VARIOUS MARTENSITIC STAINLESS STEELS WITH NEW ROBUST THERMOGRAPHIC DATA ANALYSIS.

De Finis R., Palumbo D., Ancona F., Galietti U.

Politecnico di Bari, Department of Mechanics, Mathematics and Management,
Viale Japigia, 182, 70126 Bari, Italy

rosa.definis@poliba.it, davide.palumbo@poliba.it, francesco.ancona@poliba.it, umberto.galietti@poliba.it

Corresponding author: De Finis Rosa.

Abstract

Thermography represents an important tool to study fatigue behaviour of materials.
In this work, the fatigue limit of martensitic and precipitation hardening stainless steels has been determined with thermographic methods. Despite their use in corrosive and cryogenic environments, there is a data lack in literature concerning the study of fatigue behaviour.
The peculiarity of these materials is the brittle behaviour: therefore, during fatigue tests the characteristic small deformations determine small changes of temperature. Thus, to properly determine the fatigue limit of aforementioned stainless steels, a more accurate setup is necessary in order to correctly detect surface temperature of specimens due to dissipation heat sources.
In literature, different procedures have already been proposed to evaluate the fatigue limit from thermal data but very few works lead to an early detection of dissipation process which can obtain a further reduction of overall testing time. The aim of the paper is to propose a new robust thermal data analysis procedure for estimating fatigue limit of stainless steels in automatable way.

Keywords: stainless steel, thermography, fatigue behaviour.

1. Introduction

The aim of the work is to study the fatigue behaviour of martensitic stainless steels and in particular to propose a new procedure to assess the fatigue limit with thermography in automatable way. The tested stainless steels are: X4 Cr Ni Mo 16-5-1, ASTM A 182 F6NM, AISI 422 (with martensitic lattice), 17-4PH (precipitation hardening). The "Stair Case" method has been carried out in order to obtain a comparison with thermography results for ASTM A 182 F6NM and 17-4PH.
In recent years, thermography has been used to study fatigue behaviour of materials. In particular, temperature or thermal sources were related to the fatigue damage of material and can then be used to assess the fatigue limit [1-15].
Conventional and traditional methods generally used to obtain the fatigue limit in respect to thermographic techniques are dramatically time-consuming. For example, the "Stair case method" [16] requires more than 15 specimens and 2/3 months of a hydraulic loading machine to characterize a material, compared to maximum one week needed by thermographic techniques.

Moreover, the analysis of fatigue damage with thermal methods can provide additional information about the position and dimension of cracks and plasticization area of material [1-13].
In literature, the analysis of fatigue damage with thermography has been performed considering different approaches that can be summarized as follows:

- measurement and monitoring of the superficial temperature [3-4],[8-13].
- evaluation of the thermal heat sources (dissipative sources evaluation)[1-2],[14-15],[17].
- evaluation of the thermoelastic sources and phase thermoelastic signal (TPA method) [7-9]

In Luong's work [1] an energetic approach was used to describe the heat production mechanism correlated to intrinsic dissipation in material. Monitoring temperature variations during the test, it is possible to evaluate the dissipations and to find the fatigue limit of material by means of a graphic method.
A similar approach has been proposed by Morabito *et al*. [3] and Risitano *et al*. [4]. It is based on a suitable procedure in which the specimen is subjected to stress amplitudes which are gradually increased until failure. When the stress amplitude is higher than fatigue limit, surface temperature of the specimen increases and then reaches a plateau value. The fatigue limit of material can be assessed either considering the heating rate ($\Delta T/\Delta N$) or the steady-state temperature. Both procedures involve in linear regression straight lines in order to approximate thermal data and to find the fatigue limit.
Considering a local energy approach, different works are based on the evaluation of thermal sources to describe damage phenomena due to fatigue. These works [14-15], [17] consider the heat diffusion equation in order to quantify and separate dissipative and thermoelastic sources. This approach requires a great deal of informatics resources and thus time-consuming analyses.
An energetic approach has also been used in Meneghetti's work [2]. In particular, the fatigue limit of AISI 304L of notched and smooth specimens was investigated considering a theoretical model to quantify the "specific thermal energy loss" during fatigue tests. "Specific thermal energy loss" is due to thermal energy dissipated per unit volume and per cycle (Q parameter). The energy released by material as heat during a dynamic test is related to temperature, and then to fatigue behaviour.
Another way to study the fatigue behaviour of material is represented by the evaluation of thermoelastic sources. In the works of Krapez *et al*. [5] and Galietti *et al.* [8] the temperature signal is analyzed in the time domain so that the first and the second order signal frequency are used to describe the nonlinear signal contents in the temperature evolution, due to thermomechanical coupling phenomena. An innovative approach has been proposed in the works of Palumbo *et al.,* [7] and Galietti *et al.,* [8] based on TSA analysis [18-21]. In particular, the new method called TPA considers the phase of thermoelastic signal as a parameter for monitoring fatigue damage of material.
All the approaches illustrated above can be used to study the fatigue behaviour of metallic materials and composites [6], standard "dog bone" [8-9] or notched [10] specimen but also welded joints [7], [12]. However, despite these procedures representing a valid and effective method for obtaining fatigue limit, it is important to underline that generally the measurement of thermal signal is sensitive to external thermal noise sources that could compromise the results of tests [7], [10].
Examples of noise sources are environmental temperature and the elevated temperature of the grips of the hydraulic loading machine. The importance of these noise sources could become significant in the case of low heat sources produced by fatigue damage phenomena. This is the case of stainless steels studied in this work (martensitic and precipitation hardening steels) characterized by brittle behaviour associated with low deformations.
When such conditions occur, the methods used in literature to evaluate the fatigue limit could lead to ambiguous results. In fact, most methods propose a procedure based on linear regression of thermal data at the beginning of the test and for the last steps for which energy dissipation is clear and evident.

Only few works, [9], [11] have proposed an automatic and iterative method. In particular, the method proposed by Curà *et al*., [11] requires choosing a trial stress value that divides data in two different series: above and below fatigue limit, respectively. The intersection of straight lines interpolating data, gives the value of beginning damage. The iteration steps are repeated until the iteration error between the two stress values mentioned (one chosen and one obtained by intersection) is minimized.
Another important issue is that all the methods in literature need to bring the specimen to failure. Moreover, the quality of the results of all these methods strongly depends on the number of available data with load higher than fatigue limit. This means that the result is not univocally determined.
In this work, fatigue behaviour of martensitic stainless steels is studied by detecting surface temperature of dog bone specimens. Temperature data are processed for evaluating fatigue limit with new robust analysis.

2. Materials and specimen geometry

Four stainless steels were used in this work, X4 Cr Ni Mo 16-5-1, AISI 422 and ASTM A 182 grade F6NM with martensitic lattice and precipitation hardening type 17-4PH. Martensitic stainless steels have a higher mechanical strength obtained by a quenching heat treatment but limited corrosion resistance. In X4 Cr Ni Mo 16-5-1 (σ_{UTS} =850 MPa [22]) and ASTM A 182 grade F6NM (σ_{UTS} =650 MPa [23]), the addition of Chromium (11-16% in weight) allows for improvement of corrosion resistance through the formation of oxides, and it also allows for avoidance of the depleting of Chrome from lattice [24]. In AISI 422 (σ_{UTS}=880 MPa [22]) the percentage of chromium is 11-13 % in weight, and moreover, the presence of W, V and Mo alloys in the lattice, favors the complex carbide precipitation. So, this steel can be tempered at a relatively high temperature (650 °C) without having chromium-depletion of the lattice. It is a standard type of martensitic stainless steel [25].
17-4 PH (σ_{UTS} =1365 MPa [22]) is a typical martensitic precipitation hardening stainless steel. By applying suitable heat treatments, a wide range of mechanical properties can be obtained [26].
The specimens (three in number) were used with dimensions according to ASTM E 466-96 geometry [27]. In figure 1 the most important dimensions of specimen are reported: nominal gauge length, nominal thickness and nominal width.

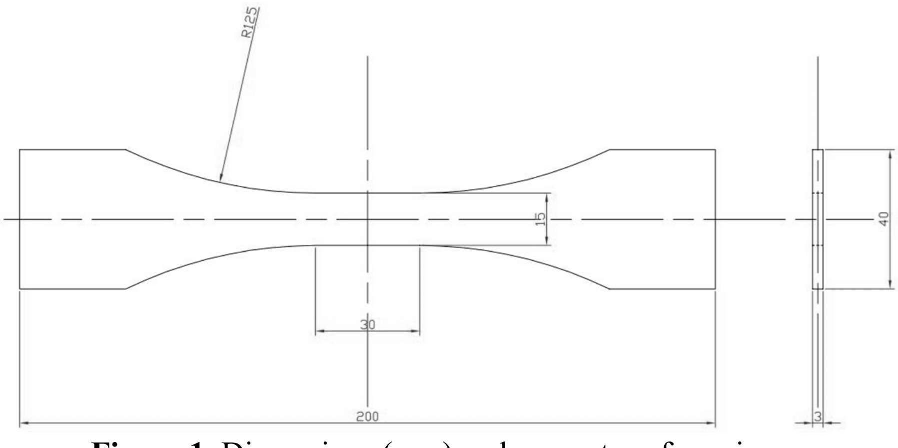

Figure 1. Dimensions (mm) and geometry of specimens

3. Experimental setup : Instruments and test procedures

The tests were carried out with the MTS model 370 servo hydraulic fatigue machine with a 100 kN capacity. The IR camera FLIR SC 640 was used to obtain thermal data. It is based on a microbolometric detector (640x480 pixels) with a thermal sensitivity NETD < 30 mK.
Specimens were sprayed with flat black spray to increase emissivity to 0.92 and they were also enclosed in an insulating chamber to avoid heat reflections due to eventual external heat sources. A painted unloaded aluminum plate acting as a black body was used to monitor the environmental temperature inside the insulating chamber, (figure 2 (a), (b)).

(a) (b)

Figure 2. (a) Loading machine, insulated chamber, specimen (b) Inside of insulated chamber: specimen, black body and IR camera.

The test consists of a stepped loading procedure sequentially applied to the specimen (Tab. 1) with a load characterised by stress ratio R=0.5 and frequency 17 Hz. Each load step lasts for 20,000 cycles [8]. The load was increased up to the point of failure of material.
The procedure requires at least 5 load steps below the fatigue limit (σ_L) of material. The authors recommend starting with a stress amplitude value ($\Delta\sigma/2$) of no more than 10% of ultimate tensile strength (σ_{UTS} [22],[23]) and completing the remaining steps increasing the stress amplitude by less than 20 MPa.
At the end of each step, mean and amplitude of the applied load was increased according to values shown in Table 1. Thermal data were acquired during the entire test with a frequency of 0.1 frames per second.

Loading step	AISI 422 Δσ/2 [MPa]	17-4 PH Δσ/2 [MPa]	ASTM A 182 F6NM Δσ/2 [MPa]	X4 Cr Ni Mo 16-5-1 Δσ/2 [MPa]
1	80,0	140,0	25,0	25,0
2	100,0	160,0	45,0	45,0
3	125,0	170,0	65,0	65,0
4	130,0	180,0	85,0	85,0
5	135,0	185,0	100,0	105,0
6	137,5	190,0	115,0	120,0
7	140,0	195,0	130,0	135,0
8	142,5	200,0	140,0	150,0
9	145,0	205,0	150,0	165,0
10	147,5	210,0	160,0	180,0
11	150,0	215,0	170,0	190,0
12	152,5	220,0	175,0	200,0
13	167,5	225,0	180,0	207,5
14	182,5	235,0	185,0	215,0
15	197,5	250,0	190,0	222,5

Table 1. Loading table in terms of stress (semi-amplitude Δσ/2): the first specimen of each material.

4. Description of IR data processing

The thermal sequence acquired during the test has been analyzed with a new procedure in order to evaluate the superficial temperature correlated with fatigue dissipation of materials.
During a fatigue test, if the load is higher than the endurance limit, temperature trend will manifest characteristic behaviour as shown in fig.3. The superficial temperature, during early cycles of load step, increases (this is called "first phase") then it remains constant (phase 2) and before failure temperature dramatically increases (phase 3) [4]. In the same figure, different trends which refer to different loads are shown.

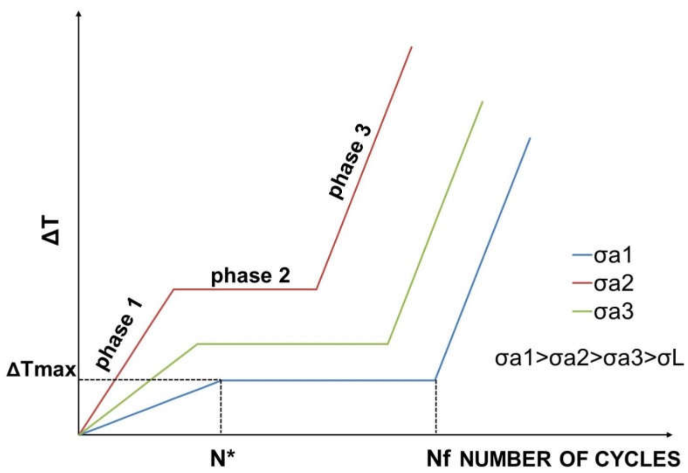

Figure 3. Expected temperature trend during a fatigue test at different load stress values above fatigue limit.

The referenced temperature analysed in all proposed methods is the plateau value ΔT_{max} in fig 3.

As just explained in the previous paragraphs, temperature changes during a fatigue test are due to dissipative sources resulting from damage phenomena. However, other external heat sources can cause variations of superficial temperature of specimen. In fact, the environmental temperature and the heating produced by the loading machine contribute to a superficial temperature increase of specimen. So, in the gauge area of specimen, the temperature T for a generic pixel with coordinates (x, y), can be expressed by the following equation:

$$T(x,y,t) = f[T_d(x,y,t), T_{amb}(t), T_{lm}(x,y,t)] \quad (1)$$

where t is a fixed time instant, T_d indicates the temperature increment due to dissipation phenomena, T_{lm} is the temperature increment effect due to continuous heat flow transferred from loading machine to specimen and T_{amb} is the environmental temperature. The only temperature change correlated to damage phenomena T_d for brittle or high conductive materials can have the same order of magnitude as the other effects becoming difficult to assess.

The proposed procedure is capable of filtering most of the external heat sources that can compromise the correct measurement of dissipative sources.

Figure 4 shows a thermographic image acquired at a given time during the loading step 13/15 (corresponding to $\Delta\sigma/2$=180 MPa) and related to specimen 1 of martensitic steel ASTM A 182 grade F6NM. Areas A_1 and A_2 refer – respectively - to the specimen gauge area, and black body area used for evaluation of the environmental temperature. T_{amb} represents the temperature mean value measured on the black body in the A_2 area. To take into account the influence of environmental conditions, T_{amb} has been subtracted from temperature T into A_1 matrix, pixel by pixel.

Temperature trend along a generic profile p (figure 4), shows the effect of hot oil in the cylinder of the loading machine. This heat is transferred by the loading machine to the specimen through the grips and it is not constant but increases during the test. Typically, when dissipative phenomena occur, a non-symmetrical thermal profile appears, figure 4 (b - c).

If a profile along the specimen p is plotted when there is only external heat and no inner heat source due to damage (fig 4b), the temperature along the specimen varies linearly from the hottest (bottom) to the coolest (upper) part. As first approximation, even with significant heat dissipation from the specimen (fig 4c), the contribution of the loading machine T_{lm} was then considered linear.

Of course there will still be an effect, even if dramatically reduced, of heating from the loading machine due to the time delay between the specimen (directly connected with the heat source) and the black body (that will heat up due to environmental change of temperature in the insulating chamber). In fact, even with evident absence of dissipation heat source (fig. 4b) there is a $\Delta T_{\_p}$ slightly different from the expected zero value. This effect will be filtered in the next step.

A straight line was used to assess T_{lm} that connects two values on the boundary of the p profile obtained substituting the central value of the first and last set of five pixels, respectively with their mean values.

The effect of T_{lm} was filtered out for each profile along the specimen in the analysis area $A1$.

Compared with other kinds of filters - as physical filters, for instance - this has the advantage of being straightforward and very simple to implement, giving equally good results.

Referring to fig. 4(b-c), the trends of unfiltered thermal profiles tend to overestimate the value of $\Delta T_{\_p}$ compared to filtered data.

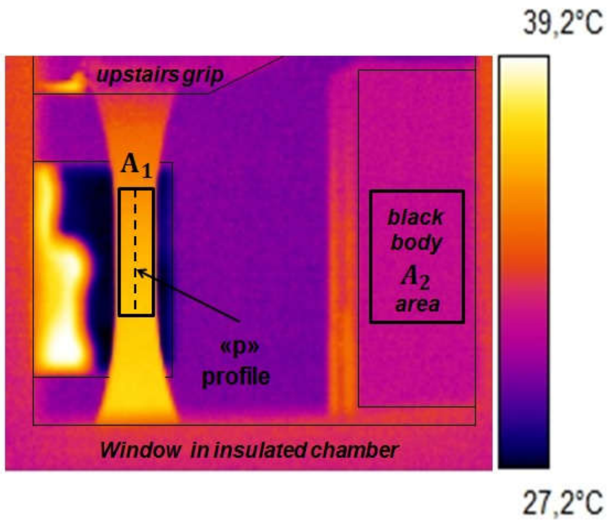

(a)

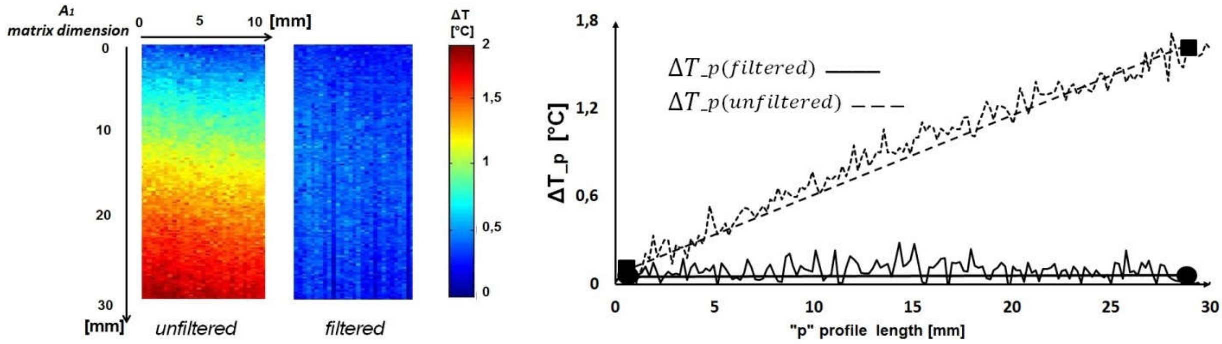

(b)

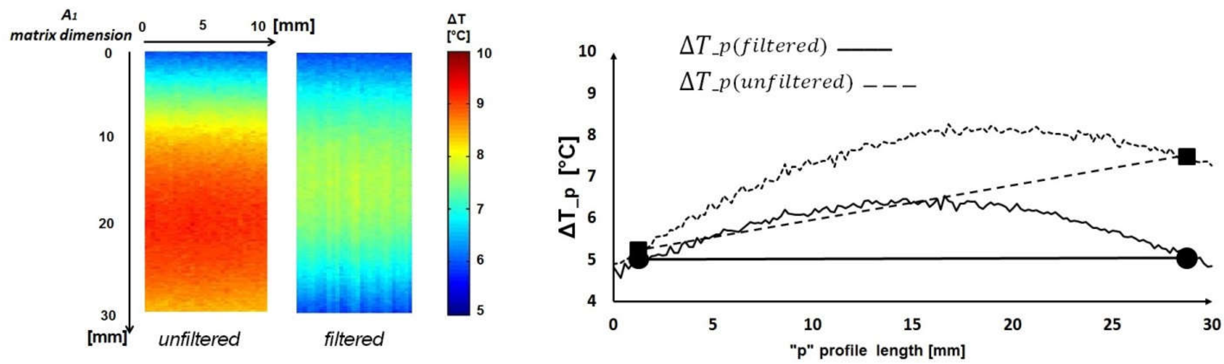

(c)

Figure 4. a) Areas and thermal profile "p" considered for analysis (ASTM A182, specimen 1): b) temperature trend along "p" profile at load step 8 (140 MPa), c) temperature trend along "p" profile at load step 13 (180 MPa).

The ΔT_{max} (figure 5) considered in this work is obtained as the maximum of the $\Delta T_{\_p}$ of the analysed A_1 area. The thermal data are represented as function of stress semi-amplitude ($\Delta\sigma/2$) imposed during fatigue test comparing unfiltered and filtered data for both ASTM A 182 and X4 Cr Ni Mo 16-5-1 (fig. 5 (a), (b)). Referring to [4], unfiltered data trend were obtained by subtracting the environmental temperature from the steady state temperature ΔT_{max} achieved during each step. All data are characterized by two different trends related to two different behaviours of material. The first steps of fatigue test are placed below the fatigue limit so no damage occurs to materials and the temperature variations detected are negligible. When damage phenomena occur, a significant temperature increase variation is observed. This behaviour can be approximately represented with a linear function that relates the temperature variations to the level of stress of material.

As shown in this paragraph, an inaccurate evaluation of all heat sources involved in the measurement of temperature could compromise the correct evaluation of the dissipative heat sources linked to fatigue damage phenomena. Moreover, some problems might occur in the evaluation of fatigue limit of material.

The flow chart in figure 6 summarizes the procedure above described.

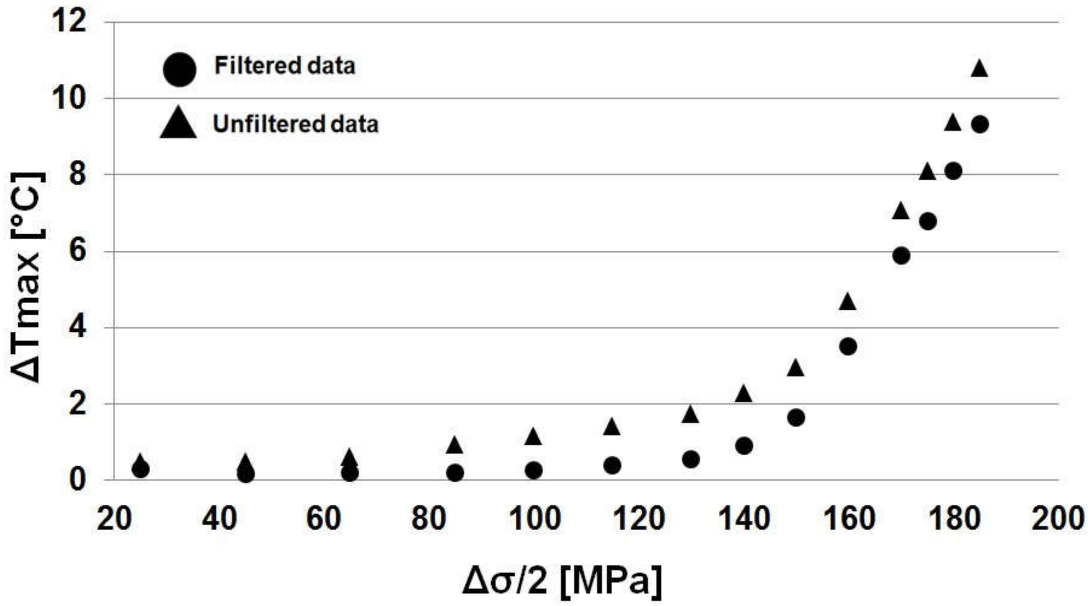

(a)

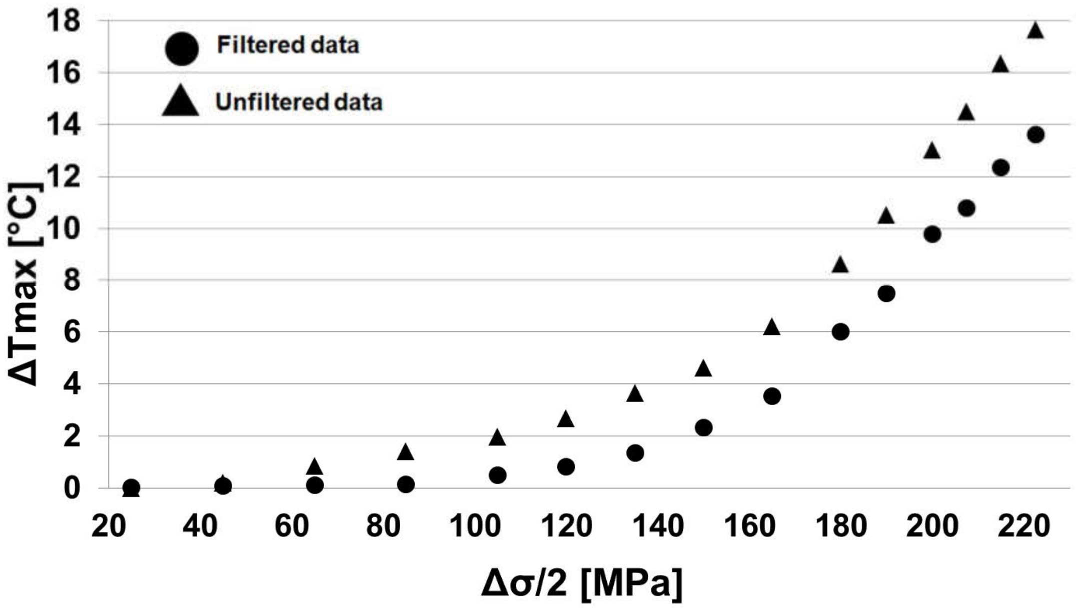

(b)

Figure 5 (a). Filtered and unfiltered temperature data, specimen 1, ASTM A 182 grade F6NM, **(b).** Filtered and unfiltered temperature data, specimen 1 X4 Cr Ni Mo 16-5-1.

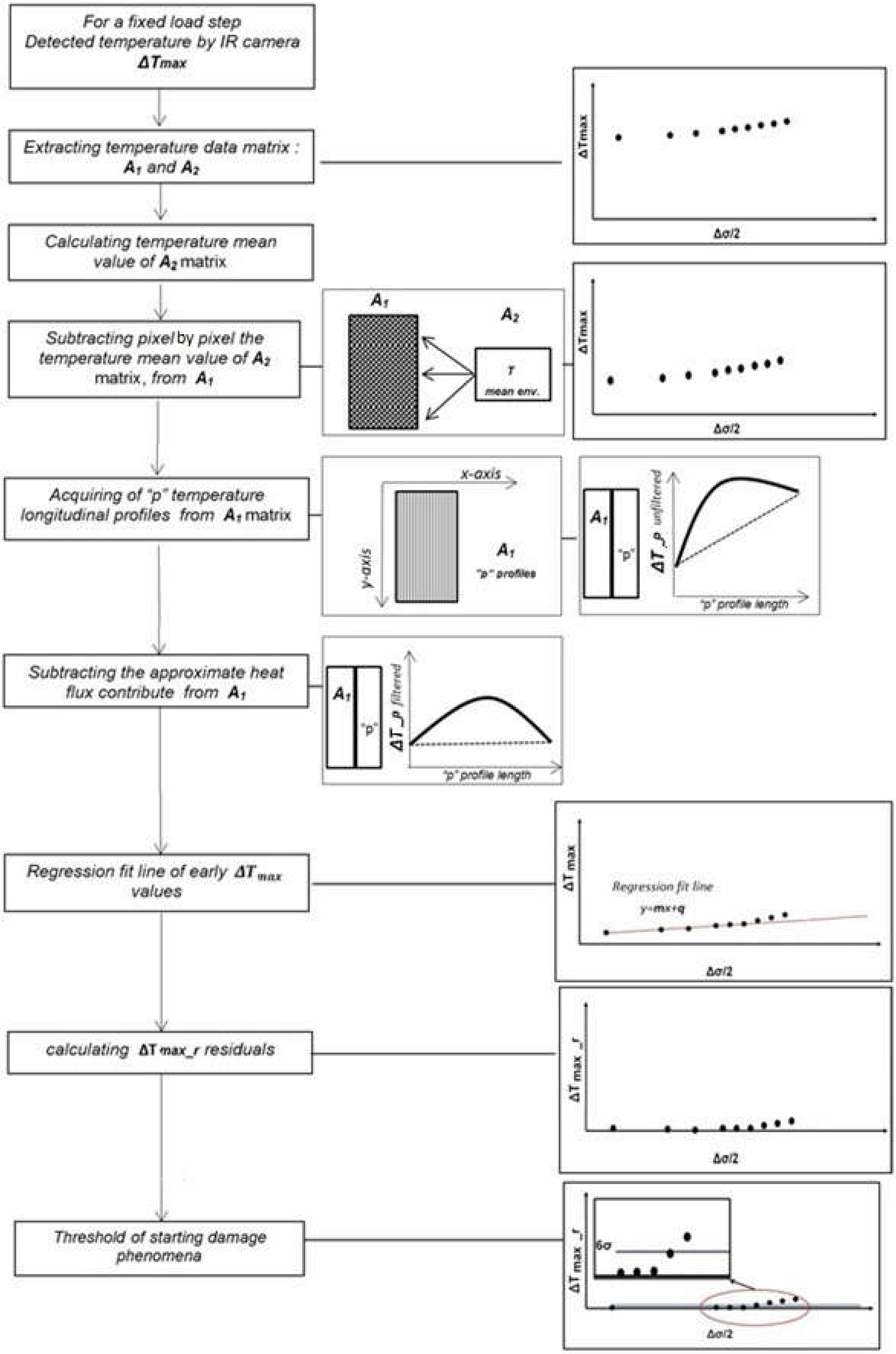
For a fixed load step
Detected temperature by IR camera
ΔTmax
Extracting temperature data matrix :
A1 and A2
Calculating temperature mean value of A2 matrix
Subtracting pixel by pixel the temperature mean value of A2 matrix, from A1
Acquiring of "p" temperature longitudinal profiles from A1 matrix
Subtracting the approximate heat flux contribute from A1
Regression fit line of early ΔTmax values
calculating ΔT max_r residuals
Threshold of starting damage phenomena
ΔTmax
Δσ/2
A1
A2
T
mean env.
x-axis
y-axis
"p" profiles
"p"
ΔT_p unfiltered
"p" profile length
ΔT_p filtered
Regression fit line
y=mx+q
ΔT max
ΔT max _r
6σ

Figure 6. Scheme of proposed analysis procedure.

The proposed method allows for assessment of the stress amplitude value for which damage phenomena in material become statistically significant in terms of temperature change. This stress value will be characterized by a $\ddot{A}T_{max}$ statistically different from those obtained in the first 5 steps and it represents an estimate of the fatigue limit.

The method is applied on ΔT_{max} data evaluated for each value of $\Delta\sigma/2$ and consists of the following phases (figure 6):

1. linear regression analysis of the first 5 couples of data (ΔT_{max}; $\Delta\sigma/2$) and evaluation of the best fit line($y=mx+q$).
2. evaluation of residuals of ΔT_{max} (ΔT_{max_r}) for each step by means of the following equation:

   $$(\Delta T_{\max\_r})_i = (\Delta T_{\max})_i - \left[m(\Delta\sigma/2)_i + q\right] \qquad \textit{for } i=1, 2, \ldots\ldots N \quad (2)$$

   where N is the number of the loading steps.
3. evaluation of standard deviation ($\sigma_{\Delta Tmax\_r}$) of residuals (ΔT_{max_r}) of the first 5 data of all tests (in this case 3 specimens and then a total of 15 data).
4. evaluation of the threshold value $\Delta T_{h\_6\sigma}=6*\sigma_{\Delta Tmax\_r}$.
5. evaluation of the first loading step (or ΔT_{max_r} data) for which the condition $(\Delta T_{max\_r})_N>\Delta T_{h\_6\sigma}$ is verified. From this loading step, the fatigue damage is considered to be statistically significant. The value of $\Delta\sigma/2$ in correspondence with this loading step provides an estimate of fatigue limit (σ_L).

For instance, in table 2 thermal data relative to ASTM A 182 grade F6NM are present, obtained by the filtering procedure. For each specimen, the constants m and q were evaluated. In table 2 the residuals used to calculate the values $\sigma_{\Delta Tmax\_r}$ and $\Delta T_{h\_6\sigma}$ are shown. In this way - for example - the value of ΔT_{max_r} statistically significant for the specimen 1 is 1,44 and the fatigue limit is 150 MPa. Figure 6 and 7(b) show the above in graph form.

		specimen 1		specimen 2		specimen 3			
N	*Δσ/2 [MPa]*	*ΔT_{max} [°C]*	*ΔT_{max_r} [°C]*	*ΔT_{max} [°C]*	*ΔT_{max_r} [°C]*	*ΔT_{max} [°C]*	*ΔT_{max_r} [°C]*	$\sigma_{\Delta Tmax\_r}$ [°C]	$\Delta T_{h\_6\sigma}$ [°C]
1	25	0,29	0,06	0,94	0,25	0,7	0,07		
2	45	0,17	-0,05	0,4	-0,21	0,6	-0,04		
3	65	0,19	-0,03	0,36	-0,17	0,54	-0,1	0,12	0,72
4	85	0,2	-0,02	0,38	-0,07	0,64	-0,01		
5	100	0,27	0,05	0,6	0,21	0,72	0,07		
6	115	0,38	0,17	0,78	0,45	0,83	0,18		
7	**130**	0,55	0,34	1,23	**0,96**	1,1	0,44		
8	**140**	0,9	0,69	1,39	1,16	1,46	**0,8**		
9	**150**	1,65	**1,44**	2,16	1,97	2,13	1,47		
10	160	3,52	3,32	3,81	3,66	3,97	3,31		
11	170	5,89	5,68	5,96	5,85	6,39	5,72		
12	175	6,79	6,59	7,34	7,25	7,43	6,76		
13	180	8,12	7,92	9,07	9	8,43	7,76		
14	185	9,34	9,13	9,98	9,93	10,03	9,36		
m		**$-1{,}7 \cdot 10^{-4}$**		**$-4 \cdot 10^{-3}$**		**$2{,}6 \cdot 10^{-4}$**			
q		**0,23**		**0,79**		**0,62**			

Table 2. Thermal data of ASTM A 182 grade F6NM, specimen 1 after processing: graphic parameters : *m, q ; t*emperature residuals ΔT_{max_r}*;* standard deviation of residuals ,$\sigma_{\Delta Tmax\_r}$; threshold value $\Delta T_{h\_6\sigma}$ for evaluating fatigue limit.

5. Discussion of results.

In this paragraph a comparison between “traditional graphic method” [1] and the proposed procedure for thermal data analysis and subsequent evaluation of fatigue limit was performed. For 17-4 PH material and ASTM A182 a “stair case” test has been carried out with a run-out limit of 10^7 cycles in order to obtain a comparison with the classic procedure.
Figure 7 shows an example of estimation of fatigue limit on ASTM A 182 grade F6NM, specimen 2 with the two procedures just presented. In particular, figure 7 (a) shows Luong’s method [1] while figure 7 (b) shows in graph form the procedure exposed in the previous paragraph. As shown in fig. 7(b), it is not necessary to bring the specimen to failure to evaluate endurance fatigue limit.
All the results are summarized in tables 3-6 for each material. Comparable results were obtained between the two thermographic methods used. However, the proposed method allows for an early-stage automatic and univocal determination of the fatigue limit.
Differences were obtained between thermal data and the Stair Case method. In particular, the fatigue limit obtained with thermal data is lower than with the Stair Case method for all tested materials. Such difference can be attributed to run-out cycles imposed to choose the fatigue limit. In fact, for steels including martensitic lattice types (such as 17-4PH) [28] there is a difference between the fatigue limit evaluated at 10^7 and 10^9 cycles (around 100-200 MPa). Therefore, thermal dissipations seem linked to damage fatigue phenomena that can occur for load levels lower than endurance evaluated at 10^7.

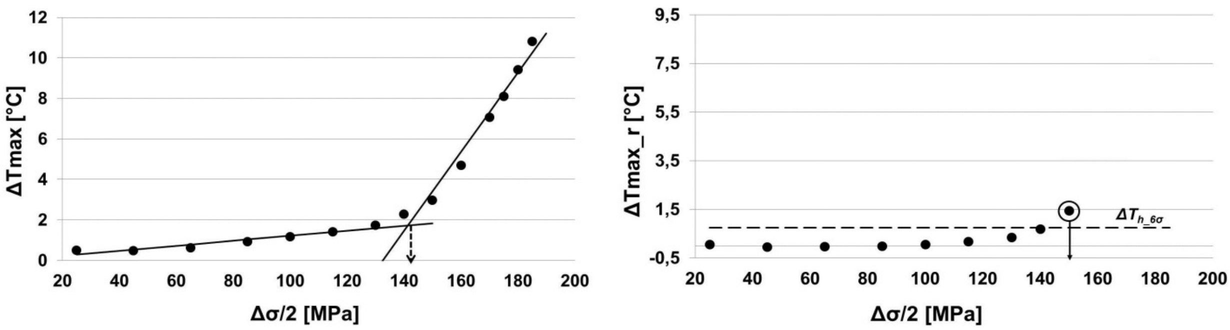

(a) ***(b)***

Figure 7. Fatigue limit evaluation: (a) Comparison between Luong's method and (b) proposed method, ASTM A 182 grade F6NM, specimen1.

Specimen	Traditional Graphic Method (σ_L) [MPa]	Proposed Method (σ_L) [MPa]	Stair Case Method (σ_L) [MPa]
1	141,4	150,0	
2	146,0	130,0	
3	129,3	140,0	
Average	**138,9**	**140,0**	**169,3**
Standard Deviation	**8,6**	**10,0**	**4,4**

Table 3. ASTM A 182 F6NM fatigue results: comparison between graphic and proposed methods.

Specimen	Traditional Graphic Method (σ_L) [MPa]	Proposed Method (σ_L) [MPa]	Stair Case Method (σ_L) [MPa]
1	207,7	200,0	
2	200,2	200,0	
3	207,0	205,0	
Average	**205,0**	**201,7**	**212,1**
Standard Deviation	**4,1**	**2,9**	**3,8**

Table4. 17-4 PH fatigue results: comparison between graphic and proposed methods.

Specimen	Traditional Graphic Method (σ_L) [MPa]	Proposed Method (σ_L) [MPa]
1	129,2	142,5
2	127,8	145,0
3	139,2	140,0
Average	**132,1**	**142,5**
Standard Deviation	**6,2**	**2,5**

Table 5. AISI 422 fatigue results: comparison between graphic and proposed methods.

Specimen	Traditional Graphic Method (σ_L) [MPa]	Proposed Method(σ_L) [MPa]
1	157,8	150,0
2	154,4	150,0
3	142,8	165,0
Average	**151,7**	**155,0**
Standard Deviation	**6,4**	**8,7**

Table 6. X4 CR NI MO 16-5-1 fatigue results: comparison between graphic and proposed methods.

The proposed method leads to a new way of performing fatigue tests with thermal analysis.
As said, in many works (e.g. [1], [7],[13]) the procedure used to perform fatigue tests consists in incremental cyclic loads imposed on the specimen up to failure and the evaluation of fatigue limit takes into account, in particular, the temperature variations of the last loading steps.
By applying the proposed procedure it is possible to obtain fatigue limit avoiding specimen failure: in fact, the test can be stopped when the threshold value $\Delta T_{h\_6\sigma}$ is reached (see fig. 8b or 9b).
Moreover, a more accurate assessment of fatigue limit is possible. When the threshold $\Delta T_{h\_6\sigma}$ is reached, it is possible to refine the test decreasing the load back to the previous step and imposing smaller load increments.
As shown in tables 3-6, the proposed method provides discrete value of fatigue limit. By imposing smaller load increments - as just said - the standard deviation (which corresponds to load increment for ASTM A 182 in table 3) could decrease. This approach can improve the evaluation of fatigue limit.
The results are in good agreement with traditional graphic thermographic method used in literature. However, thermographic technique seems to underestimate fatigue limit in respect to the Stair-Case method. This is probably due to the fact that fatigue limit is conventional at 10^7 cycles (see very high cycle fatigue phenomena [28]). Further works will focus on studying and comparing of the fatigue limit at 10^7 and 10^9 cycles with both thermal and Stair Case for very high cycle fatigue.

6. Conclusion

In this work the fatigue behaviour of stainless steels has been studied by means of thermography technique. Fatigue tests were carried out on martensitic and precipitation hardening steels. These materials are characterized by a brittle behaviour and the temperature variations related to damage phenomena are one order less than austenitic steel ones. So a more accurate set up was needed in order to evaluate the superficial temperature of specimen.
A new procedure of analysis of thermographic data has been developed, capable of taking into account all the heat sources involved in fatigue tests. In particular this procedure forecasts a smoothing filter method for thermal data and a new technique for estimating fatigue limit. Moreover, an accurate measurement of temperature relative to dissipative phenomena has been performed and an automatable procedure has been proposed to determine the fatigue limit.
The results are in good agreement with traditional graphic thermographic methods used in literature. Thermographic technique seems to slightly underestimate fatigue limit in respect to the Stair-Case method.
Further works will focus on studying and comparing of the fatigue limit at 10^7 and 10^9 cycles.

The proposed procedure also represents a possible non-destructive technique that can be used for monitoring, studying and predicting the fatigue behaviour of materials. Besides, it can be exploited for the monitoring of large scale operating components.

Acknowledgement

This work is part of a large-scale research project (PON-SMATI) aimed at identifying innovative steels for turbo machinery used in extreme environmental conditions. The authors would like to thank GE oil & gas (Nuovo Pignone S.r.l.) for the support and collaboration provided in the experimental tests.

References

[1]Luong MP. Infrared Thermographic scanning of fatigue in metals. Nuclear engineering and Design. 1995;363:373-158.
[2]Meneghetti G. Analysis of the Fatigue Strength of a Stainless Steel Based on the Energy Dissipation.International Journal of Fatigue.2007;81:94-29.
[3]Morabito AE,Dattoma V, Galietti U.Energy-Analysis of Fatigue Damage by Thermographic Technique.Thermosense XXIV Conference.2002;460:467-4710.
[4]Risitano A, Risitano G. L'importanza del Parametro Energetico Temperatura per la Caratterizzazione Dinamica dei Materiali. Frattura ed Integrità Strutturale; 2009;113:124-9.
[5]Krapez JK, Pacou D, Gardette G. Lock-In Thermography and Fatigue Limit of Metals.Quantitative Infrared Thermography,2000; 277:282-6.
[6]Kordatos EZ, Dassios KG, Aggelis DG, Matikas TE.Rapid Evaluation of the Fatigue Limit in Composites Using Infrared Lock In Thermography and Acoustic Emission. Mechanics Reserch Communication,2013; 14:20-54.
[7]Palumbo D, Galietti U. Characterization Of Steel Welded Joints By Infrared Thermographic Methods. Quantitative Infrared Thermography, 2014; 29:42-11.
[8]Galietti U, Palumbo D, De Finis R, Ancona F. Fatigue Damage Evaluation of Martensitic Stainless Steel by Means of Thermal Methods. National Conference IGF XXII, Rome. 2013; 80:90.
[9]Galietti U, Palumbo D, De Finis R, Ancona F. Fatigue limit evaluation of martensitic steels with thermal methods. QIRT Conference. 2014.
[10]La Rosa G, Risitano A. Thermographic Methodology for Rapid Determination of the Fatigue Limit of Materials and Mechanical Components. International Journal of Fatigue, 2000; 65:73-22.
[11]Curà F, CurtiG, Sesana R. A New Iteration Method For The Thermographic Determination Of Fatigue Limit In Steels. International Journal of fatigue, 2005;453:459-27.
[12]Uhmenofer T, Medgenberg J. On the Use of Infrared Thermography for the Analysis of Fatigue Damage Processes in Welded Joints.International Journal of Fatigue,2009;130:137-31.
[13]Risitano A, Risitano G. Analisi Termica per la Valutazione del Danno negli Acciai. Workshop IGF. Forni di Sopra. 2010.
[14]Morabito AE, Chrysocos A, Dattoma V, Galietti U. Analysis of heat sources accompanying the fatigue of 2024 T3 aluminium alloys. International Journal of Fatigue, 2007; 977:984-29.
[15]Boulanger T,Chrysochoos A, Mabru C, Galtier C. Calorimetric Analysis of Dissipative and Thermoelastic Effects Associated with the Fatigue Behavior of Steels. International Journal of Fatigue. 2006;221-229-26.
[16]UNI 3964. Prove meccaniche dei materiali metallici. Prove di fatica a temperatura ambiente. Principi generali. 1985.
[17]Chrysochoos A, Huon V,Jourdsan F, Muracciole JM, Peyroux R, Wattrisse B. Use of Full-Field Digital Image Correlation and Infrared Thermography Measurement for the Thermomechanical Analysis of Material Behaviour. Strain. 2009;117:130-46.
[18]Pittaresi G, Patterson EA. A review of the general theory of thermoelastic stress analysis. The Journal of Strains Analysis for Engineering Design. 2003; 38 (5):405-17.

[19]Harwood N, Cummings W. Thermoelastic Stress Analysis. New York: National Engineering Laboratory. Adam Hilger;1991.
[20]Diaz FA, Patterson EA, Tomlinson RA, Tomlison JR, Yates JR. Measuring Stress Intensity Factors During Fatigue Crack Growth Using Thermoelasticity. Fatigue Fracture Engineering Material Structure, 2004;571:583-27.
[21]Wang WJ, Dulieu-barton JM, Li Q. Assestment of non-adiabatic behavior in Thermoelastic Stress Analysis of Small Scale Components. Experimental Mechanics. 2010; 449:461-50.
[22]Web site: http://www.Matweb.com. Matweb Material Property Data.
[23] Web site: http://www.epmetals.co.uk. Exploration and Production Metals.
[24]McGuire MF. Martensitic Stainless Steels. In: M. F. McGuire, Stainless Steels for Design Engineers. Asm International; 2008, p. 123-135.
[25]Tomei R. Criteri di scelta degli acciai inossidabili in funzione degli impieghi. In: R. Tomei, La meccanica italiana;1981,p. 55.
[26]Wu JH. High-temperature Mechanical Properties, Fatigue and Fracture Behaviour of 17-4PH stainless steel.Ph.D. Thesis. 2003. Department of Mechanical Engineering, National Central University,TaiwanR.O.C.
[27]ASTM E 466-96, Standard Practice for Conducting Force Controlled Constant Amplitude Axial Fatigue Tests of Metallic Materials.
[28]I. Marines, X. Bin, C. Bathias. An understanding of very high cycle fatigue of metals. International Journal of Fatigue. 2003; 1101:1107-25.